Synthesis of Perovskite-Ceria Composites for Solar-to-Fuel Conversion

by

Neil Aggarwal

Submitted to the Department of Materials Science and Engineering
In Partial Fulfillment of the Requirements for the Degree of

Bachelor of Science

at the

Massachusetts Institute of Technology
June 2018

Signature redacted

Signature of Author.....

Neil Aggarwal
Department of Materials Science and Engineering
May 4, 2018

Signature redacted

Certified by.....

Jennifer L. M. Rupp
Thomas Lord Assistant Professor of Material Science and Engineering
Thesis Advisor

Signature redacted

Accepted by.....

Juejun Hu
Associate Professor of Materials Science and Engineering
Chairman, Undergraduate Committee

Synthesis of Perovskite-Ceria Composites for Solar-to-Fuel Conversion

By
Neil Aggarwal

Submitted to the Department of Materials Science and Engineering
In Partial Fulfillment of the Requirements for the Degree of Bachelor of Science

Abstract

Finding suitable replacements for fossil fuels is key to a more sustainable energy economy. This thesis investigated the effectiveness of novel composite materials made from previously researched state-of-the-art materials as catalysts in the thermochemical solar-to-fuel conversion process. Materials such as ceria and gadolinium-doped ceria (GDC) have been determined to have excellent kinetics for this process but have a very high operating temperature. In contrast, perovskites have the advantage of a lower operating temperature but it comes at the expense of lower production rates. Composites containing ceria/GDC/YSZ and perovskite were synthesized to explore synergies that may result in improved performance as a catalyst for the fuel conversion process. Two of these perovskite-ceria composites , LSCF-GDC and LSCC-ceria, showed promise as materials that perform better than their respective individual components. Improved fuel production and oxygen release was observed with these composites in specific temperature regimes (1000-1100°C for oxidation, 1200°C for reduction).

Thesis Advisor: Jennifer L. M. Rupp

Title: Thomas Lord Assistant Professor of Materials Science and Engineering

Acknowledgements

To Dr. Alexandar Bork, my direct supervisor and mentor, for his passion, kindness, and steadfast support. It was an absolute privilege to contribute to his ongoing work, and learn so much from him on a daily basis.

To Prof. Jennifer L. M. Rupp, whose conviction when talking about the issues our world faces with regards to energy and sustainability caught my attention to the amazing work her lab is doing. To her entire group for being so welcoming and positive. Danke Schön!

To SUMS, Angelita, Tiffany, and the entire Course 3 staff for an invigorating learning environment throughout my time at MIT.

To my friends and family, whose love and support for me mean more than anything in the world.

Contents

List of Figures

List of Tables

1. Introduction and Background

1.1 Motivation

We face two conflicting challenges in the immediate future: 1) increasing energy demand[1] and 2) the need to decrease greenhouse gas emissions. Given the enormous presence of fossil fuels in the energy industry, alternative fuel sources must provide the comparable positives that fossil fuels do, with regards to factors such as energy density and ease of storage. Solar-to-fuel thermochemical conversion serves as a potential alternative which can produce cleaner fuels that provide a comparable storability[2]. A solar-based energy source stored as a fuel also overcomes the issue of intermittent energy supply that is inherent in other methods involving solar energy[3].

1.2 Theoretical Background

Solar-to-fuel conversion is a process of converting solar energy into chemical fuel. In this thermochemical process, a metal oxide undergoes reduction at high temperature, and is then oxidized with CO_2 and H_2O at a slightly lower temperature to produce CO and H_2 to be used as fuel[4]. The high temperature for reduction is achieved by concentrated solar power. The splitting of H_2O and CO_2 during the oxidation reaction in the presence of a metal oxide catalyst occurs at a much lower temperature than achievable directly[5]. Both CO and H_2 are storable liquid fuels and provide a solution to the issue of intermittency in the availability of solar energy. The solar-to-fuel conversion cycle undergoes the following thermochemical reactions, starting with the reduction step:

$$\frac{1}{\delta} MO_2 \rightarrow \frac{1}{\delta} MO_{2-\delta} + \frac{1}{2} O_2$$

Where MO_x is the metal oxide being reduced at high temperature. The reduced metal oxide is then exposed to water and carbon dioxide at a lower temperature, undergoing the following oxidation reactions:

$$H_2O\ (g) + \frac{1}{\delta} MO_{2-\delta} \rightarrow \frac{1}{\delta} MO_2 + H_2\ (g)$$

$$CO_2\ (g) + \frac{1}{\delta} MO_{2-\delta} \rightarrow \frac{1}{\delta} MO_2 + CO\ (g)$$

The two main classes of materials investigated in this thesis (ceria and perovskites) have both been researched before to evaluate their effectiveness as catalysts in the fuel conversion process[3]. CeO_2 (Ceria) has demonstrated stability at high temperature, favorable kinetics, and high efficiency. It can handle a high concentration of oxygen vacancies after reduction while maintaining its cubic fluorite crystal structure[7]. Two shortcomings of the material relevant to this topic include: 1) a high requisite temperature for reduction (1500°C) and 2) low oxygen non-stoichiometry (δ).

Along with ceria, gadolinium-doped ceria (GDC) and yttrium-stabilized zirconia (YSZ) were used to synthesize composites with perovskites in this thesis. Doping ceria with gadolonium has been shown to affect its behavior in oxidation, enhancing reduciblity[7].In past work investigating composites with YSZ, it was shown that the material contributed to improved thermal reduction[8].

Perovskite oxide materials, categorized by the ABO_3 structure seen below (Figure 1-1), have also been investigated as a promising catalyst for this process[3]. Perovskites have been used in several applications, including batteries, photovoltaic electrodes, dielectrics, etc.[5] The perovskite structure is energetically stable, and its ability to accommodate several elements on the periodic table means that its catalytic and electrochemical properties are very tunable.

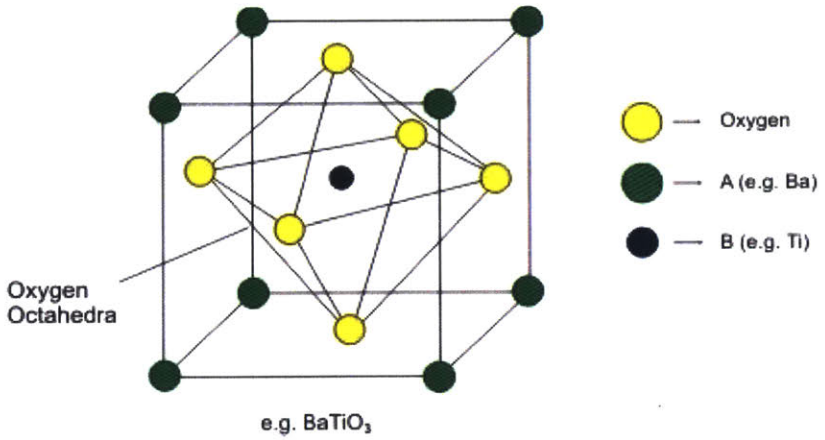

Figure 1-1. Structure of Perovskite material.

In comparison to ceria, perovskite oxides have a lower operating temperature range (800-1200°C), but that also sluggish kinetics. Perovskite oxides have generally demonstrated high oxygen release in the initial reduction step but low oxidation levels in the second step. The peak fuel production rates for perovskites (0.06-0.60 mL_{fuel} / min / g_{oxide}) are considerably lower than the rates measured for ceria (up to 12.5 L_{fuel} / min / g_{oxide})[4].

Here, composites of these two classes of materials are synthesized and investigated to determine if synergies can be attained. The aim was to find a composite that would keep the fast kinetics inherent in Ceria/GDC while attaining higher oxygen release evident in perovskites, as well as have enhanced reducibility in comparison to composites with YSZ. Three perovskite oxide series will be utilized: $(La_{0.65}Sr_{0.35})_{0.95}MnO_{3\pm\delta}$ (LSM), $La_{0.6}Sr_{0.4}Cr_{0.2}Fe_{0.8}O_3$ (LSCF), and $La_{0.6}Sr_{0.4}Cr_{0.8}Co_{0.2}O_3$ (LSCC). Prior work[5] has reliably established thermodynamic properties for LSM, while LSCF is being investigated due to its high oxygen non-stoichiometry[9] and is being widely tested as a cathode material. LSCC has been determined to produce fuel yields comparable to that of ceria, which as a perovskite makes the material very appealing for further testing[3].

2. Materials and Methods

2.1 Synthesis of LSCC Perovskite

The Pechini synthesis method[10] was used to synthesize 10g of LSCC ($La_{0.6}Sr_{0.4}Cr_{0.8}Co_{0.2}O_3$) perovskite starting with the following nitrate compounds:

Table 2.1: Components of LSCC Material

Lanthanum (III) nitrate hexahydrate	$LaNa_3O_9 \cdot 6\ H_2O$
Strontium nitrate	$Sr\ (NO_3)_2$
Chromium (III) nitrate, 98.5%	$Cr\ (NO_3)_3 \cdot 9\ H_2O$
Cobalt (II) nitrate hexahydrate	$Co\ (NO_3)_2 \cdot 6\ H_2O$

These nitrate compounds (amounts measured to obtain listed stoichiometry) were stirred together in a beaker with water. Citric acid (CA) and ethylene glycol (EG) were mixed into the beaker, with the ratio of CA and the total metal cation being 1.5 and the ratio of CA and EG being 1.5 wt%. This mixture was heated at 120°C until a viscous gel formed. This gel was calcined at 500°C, and heat treated for 5 hours at 1400°C. The sample was characterized using XRD to verify that no unwanted phases were formed.

2.2 Synthesis of Perovskite-Ceria Composites

The following perovskites and other ceramics were used as components to synthesize composites in 50/50 ratios (Table 2.2):

Table 2.2: List of ceramics used to synthesize composites.

Perovskites	Other Ceramics
$La_{0.6}Sr_{0.4}Cr_{0.2}Fe_{0.8}O_3$ (LSCF)	CeO_2 (Ceria)
$La_{0.6}Sr_{0.4}Cr_{0.8}Co_{0.2}O_3$ (LSCC)	$Ce_{0.9}Gd_{0.1}O_2$ (Gadolinium-doped Ceria (10%))
$(La_{0.8}Sr_{0.2})_{0.95}MnO_{3\pm\delta}$ (LSM)[2]	$(ZrO_2)_{0.08}(Y_2O_3)_{0.092}$ (Yttrium-stabilized zirconia)

The resulting composites were: LSCF-CeO_2, LSCF-GDC, LSCF-YSZ, LSCC-CeO_2, LSCC-GDC, LSCC-YSZ, LSM-CeO_2, LSM-GDC, and LSM-YSZ.

For each composite, 1 g each of the two components (1 g LSCF and 1 g CeO_2, for instance) were placed in a beaker with enough deionized water to dissolve the powder. This beaker was sonicated for 30 minutes, and then stirred on a hot plate above 100°C until visibly dry. The beaker was then placed in a drying oven overnight to remove excess moisture. After drying, samples were calcined at 1300°C for 5 hours, and then ground to a powder for testing.

2.2 Reactor Test

For each sample, 1g of powder was poured into a 0.5 cm diameter alumina tube, with high temperature insulation wool used to securely hold the powder at the midpoint of the tube. This was to ensure that the sample is in the middle of the furnace, where the temperature is most reliably measured by thermocouples placed within the furnace. Care was taken in between experiments to clean the rod before use to ensure that no foreign material interfered with the measurements.

Once the tube was placed in the reactor, two programs were run simultaneously: a temperature program to heat the material, and a mass flow control program to inject CO_2 in periods of constant temperature. These program scripts were written in Python and were coordinated with each other to ensure that the CO_2 injections came at steady temperatures. The samples were heated to a range of temperatures, to test the effectiveness of oxidizing CO_2 in different regimes (Figure 2-1). A long time was spent heating the sample up to 1000°C in order to ensure a 'null' environment was established with flowing Argon or Nitrogen.

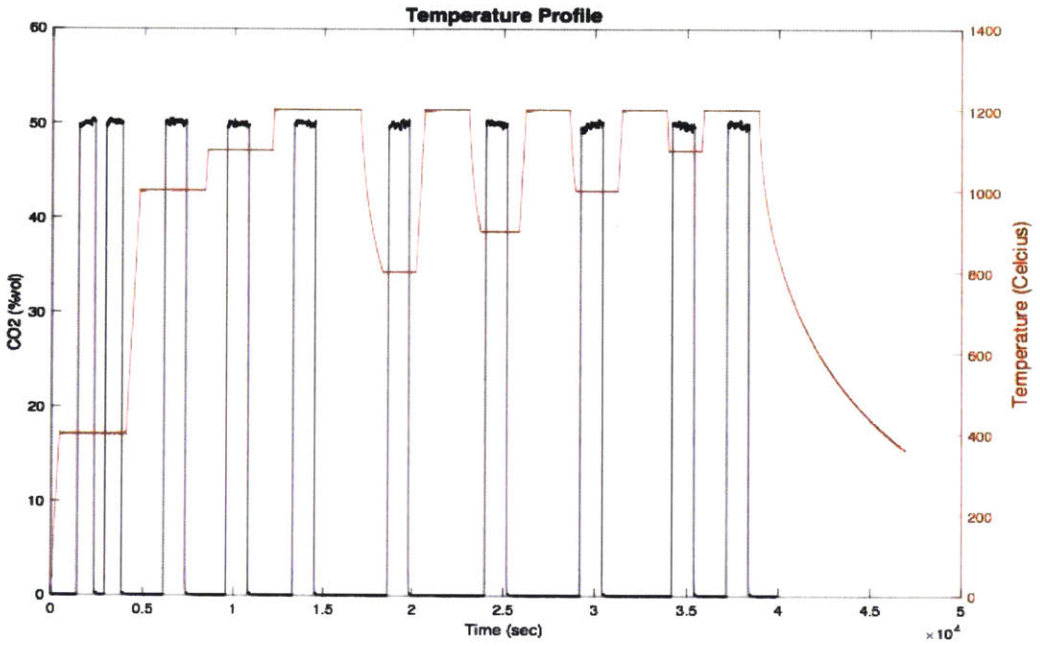

Figure 2-1: Temperature profile of reactor test. Mass Flow Control program was adjusted accordingly to ensure that CO_2 injections occurred at steady temperatures.

Whenever CO_2 was not flowing, an inert gas filled the chamber to 'reset' the environment and ensure that no residual CO_2 was reacting with the material. Ample time was placed before and after the injections to ensure steady temperature conditions.

2.3 Analysis

A Raman gas analyzer was used to measure the volume of CO relative to the total volume of gas, which at all times was flowing at 300 mL/min. Using this reference point, the amount of CO produced can be calculated for any given 'peak' indicating a 20 minute period of CO_2 flowing at 150 mL/min (50% of total flow). For a selected set of peaks, a comparison plot was made displaying the fuel production of a composite and its two individual components. Oxygen release is observed for these same peaks. From these graphs, conclusions can be made about the synergies attained in both the oxidation and reduction steps by using the composites as catalysts as opposed to its requisite components.

3. Results

3.1 Characterization

X-ray diffraction (XRD) was performed on LSCC to verify its structure before undergoing thermocycling.

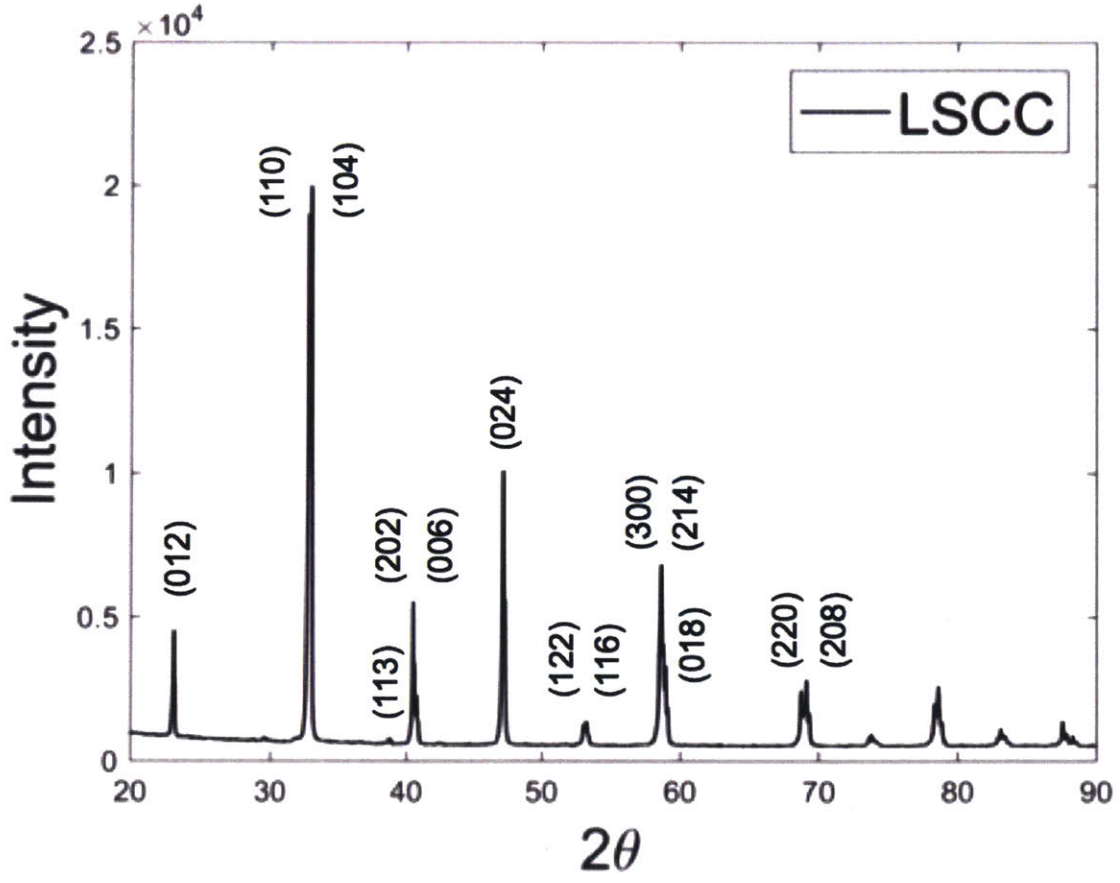

Figure 3-1. X-ray diffraction patterna of powdered $La_{0.6}Sr_{0.4}Cr_{0.8}Co_{0.2}O_3$.

Small impurities were observed at 2θ = 29.5 and 2θ = 38.5, which prompted an additional annealing treatment at 1400°C for 5 hours.

3.2 LSCF-Ceria

Table 3.1 (below) shows the amount of CO produced from each material across a range of oxidation temperatures (800°C, 900°C, 1000°C, 1100°C) in a 20 minute cycle. The reduction temperature was 1200°C for each cycle.

Table 3.1: CO Yields of CeO_2 – LSCF Material Set

Composition	$T_{Oxidation}$ (°C)	CO yield (mL/g)
CeO_2	800	70.5
CeO_2	900	96.8
CeO_2	1000	70.0
CeO_2	1100	65.7
LSCF	800	10.3
LSCF	900	20.9
LSCF	1000	27.5
LSCF	1100	49.7
LSCF-Ceria	800	34.0
LSCF-Ceria	900	21.4
LSCF-Ceria	1000	38.3

While the yields produced by the composite LSCF-Ceria are higher at each oxidation temperature, none are considerably higher enough to compare to the yields produced by ceria. The best case is seen at an oxidation temperature of 800°C, where the composite yield (34 mL/g) is close to the midway point between the yields of ceria (70.5 mL/g) and LSCF (10.3 mL/g), respectively. Looking at the oxygen release (Figure 3-2), we can determine whether this improved oxidation is met with improved reduction:

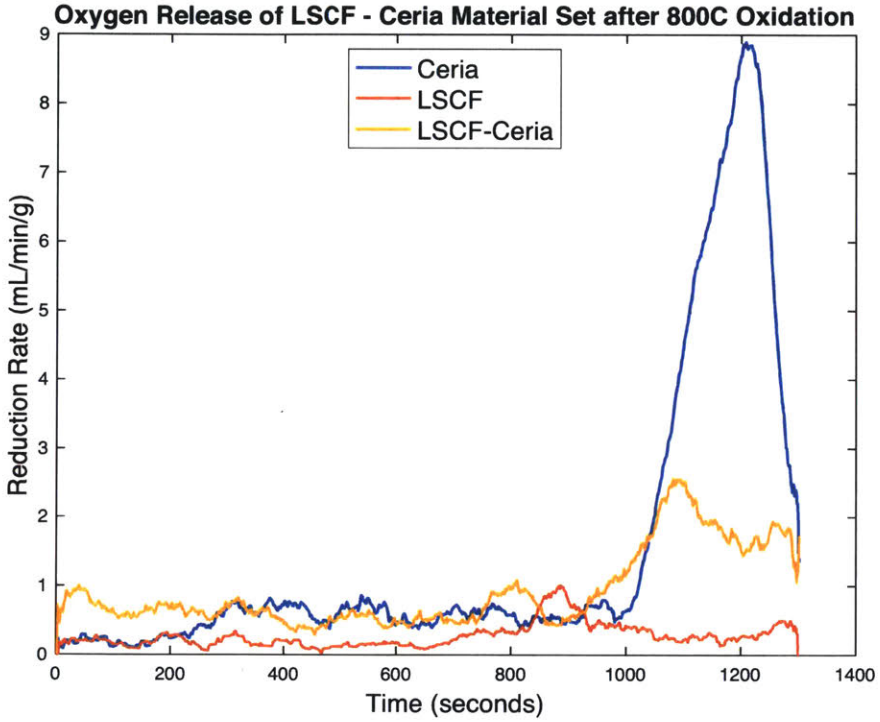

Figure 3-2. Oxygen Release of LSCF-Ceria Material Set after 800°C Oxidation. Reduction temperature of 1200°C. Set includes ceria (blue), LSCF (red), and LSCF-Ceria (yellow).

The highest reduction rate for LSCF-Ceria is considerably higher than that for LSCF. At this low oxidation temperature, however, ceria demonstrates its fast kinetics. Given that neither the improved reduction or oxidation brings the composite close to ceria's fuel production at this temperature, it is unlikely that the LSCF-Ceria (50/50) composite is useful for fuel production.

3.3 LSCF – GDC

Table 3.2 (below) shows the amount of CO produced from each material across a range of oxidation temperatures (800°C, 900°C, 1000°C, 1100°C) in a 20 minute cycle. The reduction temperature was 1200°C for each cycle.

Table 3.2: CO Yields of LSCF-GDC Material Set

Composition	$T_{Oxidation}$ (°C)	CO yield (mL/g)
$Ce_{0.9}Gd_{0.1}O_2$	800	49.2
$Ce_{0.9}Gd_{0.1}O_2$	900	50.2
$Ce_{0.9}Gd_{0.1}O_2$	1000	42.8
$Ce_{0.9}Gd_{0.1}O_2$	1100	33.5
LSCF-GDC	800	14.0
LSCF-GDC	900	23.4
LSCF-GDC	1000	44.3
LSCF-GDC	1100	77.7

At an oxidation temperature of 800°C, GDC exhibits a peak fuel production rate of 19.6 mL min^{-1} g^{-1}. Prior work[6] on samarium-doped ceria has shown peak fuel rates of 3 mL min^{-1} g^{-1} at 800°C. This large difference in fuel production for doped-cerias may be due to noise within the Raman gas analyzer, or that gadolinium-doped ceria is far superior to samarium-doped ceria.

The LSCF-GDC composite has very low fuel production at lower oxidation temperatures, but improved oxidation characteristics in the higher temperature regime (1000-1100°C). At 1100°C there is outright more CO produced by LSCF-GDC than by GDC, while at 1000°C its yield (44.3 mL/g) is greater than taking the sum of it's components, This synergy is evident for the entire cycle of fuel production (Figure 3-3):

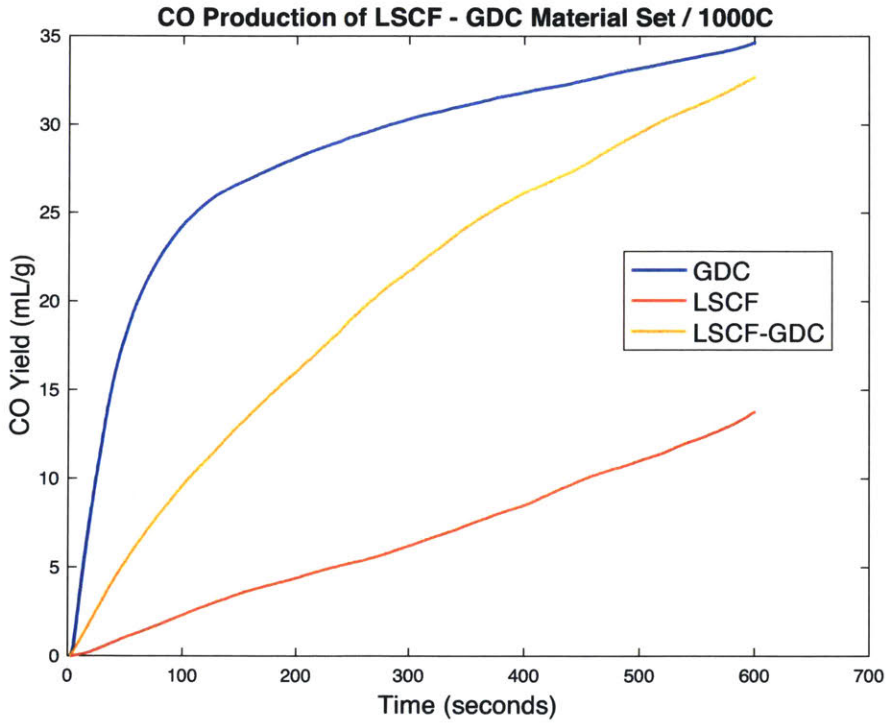

Figure 3-3. CO Yield of LSCF-GDC Material Set at 1000°C Oxidation. Set includes GDC (blue), LSCF (red), and LSCF-GDC (yellow)

The composite has an initial production rate much closer to that of GDC than LSCF, and throughout the entire cycle is producing more than the average of the two requisite components. This result in itself is a novel discovery that gives the material promise for solar-to-fuel applications. We now look at it's performance in the reduction step (Figure 3-4):

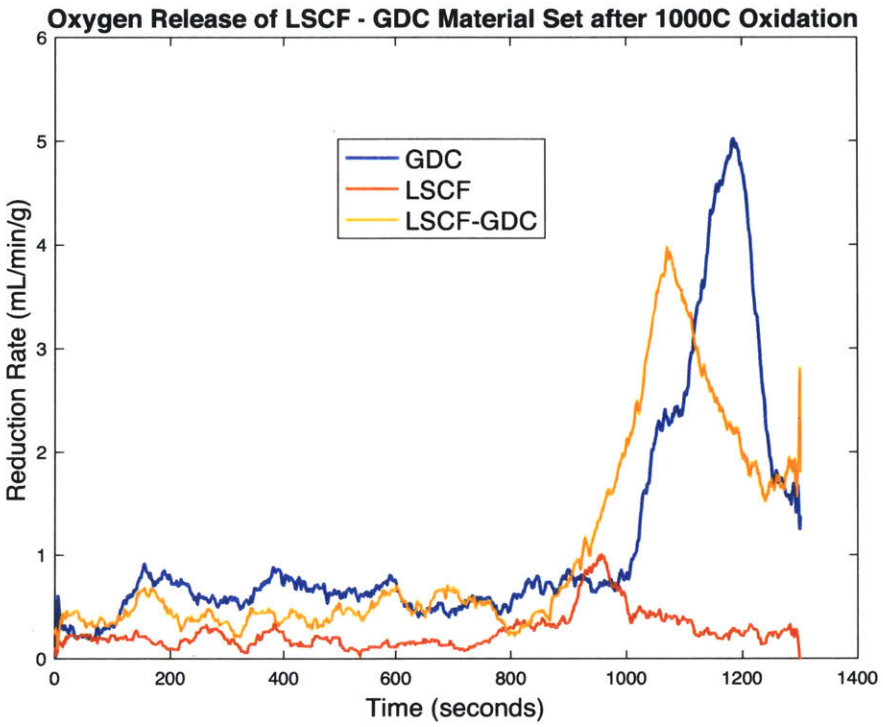

Figure 3-4. Oxygen Release of LSCF-GDC Material Set after 800°C Oxidation. Reduction temperature of 1200°C. Set includes GDC (blue), LSCF (red), and LSCF-GDC (yellow).

The LSCF-GDC composite has a reduction rate far greater than that of LSCF, and very close to that of GDC. With the improvement in fuel production and oxygen release, it is evident that this composite outperforms its components within a given temperature regime for oxidation (1000-1100°C).

3.4 LSCF-YSZ

Table 3.3 shows the amount of CO produced from LSCF-YSZ across a range of oxidation temperatures (800°C, 900°C, 1000°C, 1100°C) in a 20 minute cycle. The reduction temperature was 1200°C for each cycle.

Table 3.3: CO Yields of LSCF-YSZ

Composition	$T_{Oxidation}$ (°C)	CO yield (mL/g)
LSCF-YSZ	800	25.3
LSCF-YSZ	900	25.4
LSCF-YSZ	1000	34.3
LSCF-YSZ	1100	48.3

YSZ exhibits minimal oxidation/reduction effectiveness on its own, and thus is evaluated solely as a dopant in this research. It minimally improves the CO yield of LSCF at lower temepratures (800-1000°C) while exhibiting no change to yield at 1100°C.

3.5 LSCC-Ceria

Table 3.4 shows the amount of CO produced from LSCC-Ceria across a range of oxidation temperatures (800°C, 900°C, 1000°C, 1100°C) in a 20 minute cycle. The reduction temperature was 1200°C for each cycle.

Table 3.4: CO Yields of CeO_2 – LSCC Material Set

Composition	$T_{Oxidation}$ (°C)	CO yield (mL/g)
LSCC	900	24.2
LSCC	1000	65.6
LSCC	1100	91.4
LSCC-Ceria	1000	71.1
LSCC-Ceria	1100	105.6

Production yields at lower oxidation temperatures were minimal for both LSCC and LSCC-Ceria, and so only the higher operating temperatures are considered in this work. At 1000°C, we observe the perovskite behavior of a smaller maximum production rate but larger yield overall (Figure 3-5):

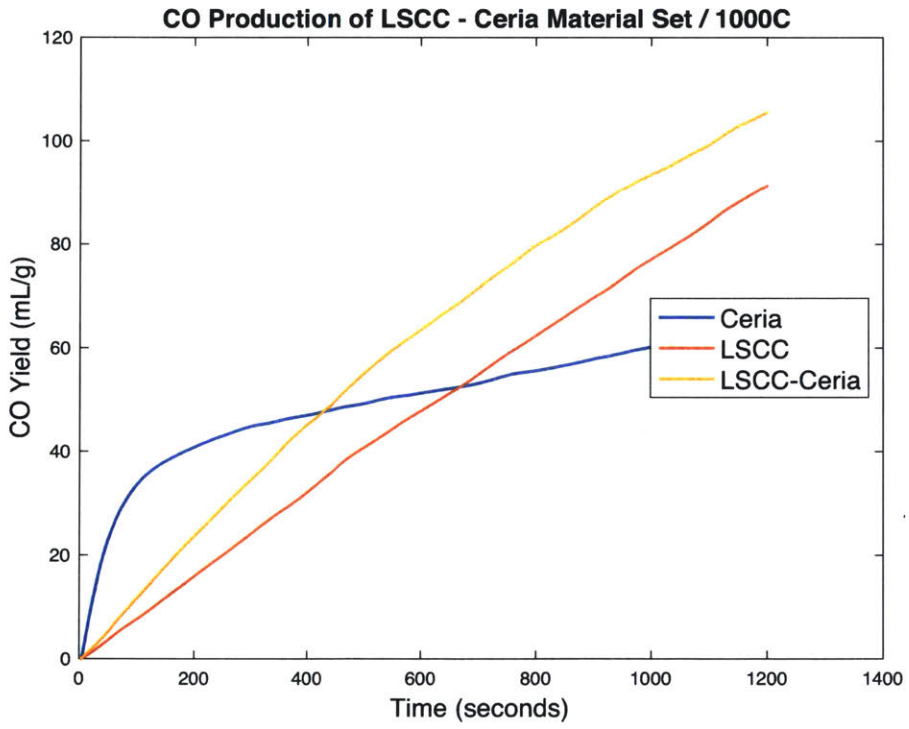

Figure 3-5. CO Yield of LSCC-Ceria Material Set at 1000°C Oxidation. Set includes Ceria (blue), LSCC (red), and LSCC-Ceria (yellow)

LSCC-Ceria outperforms both LSCC and ceria in CO production, and considerably outpaces the average yield of the two individual components.

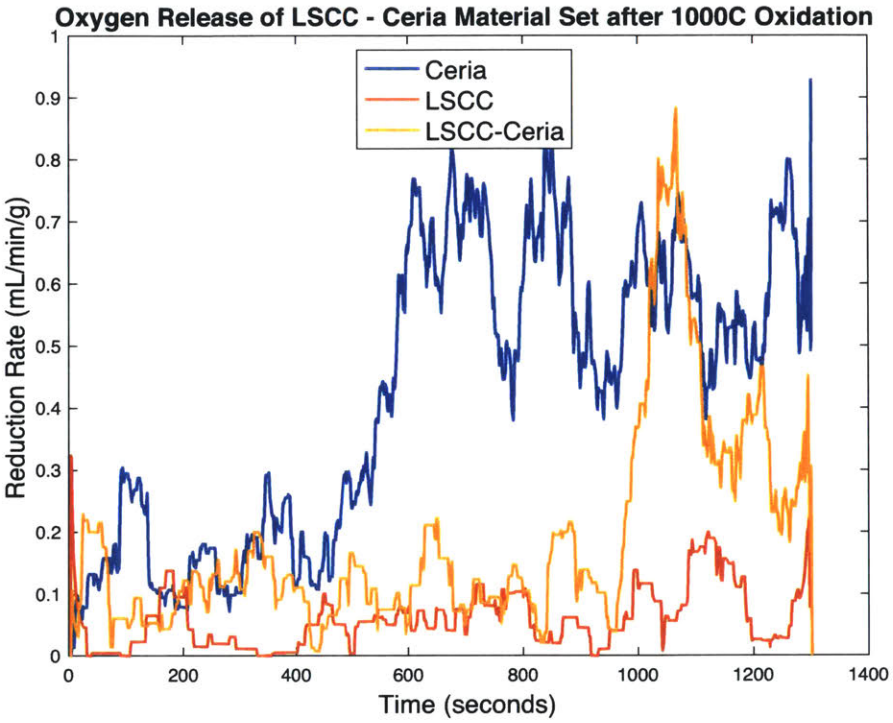

Figure 3-6. Oxygen Release of LSCC-Ceria Material Set after 800°C Oxidation. Reduction temperature of 1200°C. Set includes ceria (blue), LSCC (red), and LSCF-Ceria (yellow).

LSCC-Ceria has an oxygen release profile that more closely resembles that of Ceria. Given the higher fuel production and comparable oxygen release, this composite is effective within the 1000-1100°C temperature regime.

3.6 LSCC-GDC

While comparable to LSCC at lower oxidation temperatures, LSCC-GDC has a lower yield at 1100°C in comparison to LSCC (91.4 mL/g). The synergies observed in LSCF-GDC are not replicated using this different perovskite material.

Table 3.5: CO Yields of LSCC-GDC

Composition	$T_{Oxidation}$ (°C)	CO yield (mL/g)
LSCC-GDC	800	19.3
LSCC-GDC	900	33.5
LSCC-GDC	1000	40.8
LSCC-GDC	1100	60.3

Yields are overall lower than for LSCC-Ceria. That these two perovskite materials, LSCF and LSCC, perform better in composites with different materials, ceria and GDC (respectively), is a result worthy of further investigation.

3.7 LSCC-YSZ

As with LSCC-Ceria, CO production using LSCC-YSZ was minimal at lower reduction temperatures (800-900°C). In contrast to LSCF-YSZ, where improved production was seen at lower operating temperatures, in this composite we see a small improvement at 1100°C but no other effect.

Table 3.6: CO Yields of LSCC-YSZ

Composition	$T_{Oxidation}$ (°C)	CO yield (mL/g)
LSCC-YSZ	1000	41.8
LSCC-YSZ	1100	70.1

3.8 Isotherms

While solar-to-fuel conversion generally involves oxidation occuring at a lower temperature than reduction, it is worth observing these materials' behavior in isothermal conditions. Table 3.7 contains the CO yield for every material at 1200°C.

Table 3.7: CO Yield of every material in isothermal conditions. (Reduction/Oxidation at 1200°C)

Composition	CO yield (mL/g)
Ceria	76.3
GDC	62.0
LSCF	89.8
LSCC	118.3
LSCF-Ceria	88.2
LSCF-GDC	76.6
LSCF-YSZ	79.8
LSCC-Ceria	123.6
LSCC-GDC	90.0
LSCC-YSZ	117.6

In general we see that perovskites produce more CO than ceria and GDC. LSCC and its composites are more effective in isothermal conditions in comparison to LSCF.

4. Conclusions

4.1 Conclusions

Composites containing one component of Ceria/GDC/YSZ and one of LSCF/LSCC/LSM were synthesized to investigate synergies that result in improved performance as a catalyst for thermochemical solar-to-fuel conversion. Cycles of reduction/oxidation were conducted for each sample with reduction consistently at 1200°C and oxidation at 800°C, 900°C, 1000°C, and 1100°C. CO_2 was injected for periods of 20 minutes, and the rate and accumulation of CO was measured. Reduction and oxidation under isothermal conditions at 1200°C was also investigated.

LSCC was succesfully synthesized, with XRD characterization verifying the structure to be very similar to LSCC synthesized in previous work[3]. This sample was then used in forming composites.

Two composite materials have demonstrated syngergies between its requisite components in specific temperature regimes. LSCF-GDC has a favorable oxidation and reduction profile when being oxidized at either 1000°C or 1100°C, in comparison to its individual components of LSCF and GDC. Future work should investigate the kinetics involved in this composite, as no hypothesis on such is presented here. LSCC-Ceria also has demonstrated synergies, with a higher fuel yield at 1000°C and a substantially higher oxygen release in comparison to LSCC.

It is important to note how these synergies have been attained in very specific conditions, and that efficiency calculations have not been performed. These are required to determine whether it is beneficial to operate the material at these conditions, or if the state of the art materials previously investigated still stand as more favorable. The work presented here suggests that there are composites that strongly merit further research and consideration.

4.2 Limitations and Future Work

Without further characterization of the composite materials, particularly XRD, no conclusions can be made pertaining to the change in structure (in comparison to its individual requisite components) and how that affects the kinetics of the thermochemical conversion process. Efficiency analysis has been conducted previously for materials such as ceria[6] and would allow for comparison across several energy types in the solar space. For these materials to form a thermochemical solar-to-fuel system capable of replacing other fuel methods and methods of utilizing solar energy, evaluating the efficiency is essential.

The composite materials all were made at 50/50 ratios, while prior work on composites also investigated different ratios. While not all synergies were attained in the work presented here, it is possible that at different ratios there are better resulting properties in comparison to the components individually. Even in the two composites that show great promise (LSCF-GDC and LSCC-Ceria), there could be a more favorable composition ratio that optimizes the desireable properties of its individual components.

5. References

[1] Doman, L. "EIA Projects 28% Increase in World Energy Use by 2040." *US Energy Information Administration*, 14 Sept. 2017, www.eia.gov/todayinenergy/detal.php?id=32912

[2] Tuller, H. L. (2017) Solar to fuels conversion technologies: a perspective. *Mater Renew and Sustain Energy* **6**: 3.

[3] Bork, A. H., Kubicek, M., Struzik, M., Rupp, J. L. M. (2015) Perovskite $La_{0.6}Sr_{0.4}Cr_{1-x}Co_xO_{3-a}$ solid solutions for solar-thermochemical fuel production: strategies to lower the operation temperture. *J. Mater. Chem. A* **3**: 15546

[4] Ignatowich, M. J., Bork, A. H., Davenport, T. C., Rupp, J. L. M., Yang, C., Yamazaki, Y., Haile, S. M. (2017) Impact of enhanced oxide reducibility on rates of solar-driven thermochemical fuel production. *MRS Communications* **7**(4): 873-878.

[5] Kubicek, M., Bork, A. H., Rupp, J. L. M. (2017) Perovskite oxides - a review on a versatile material class for solar-to-fuel conversion processs. *J. Mater. Chem. A* **5**: 11983.

[6] Chueh, W. C., Haile, S. M. (2010) A thermochemical study of ceria: exploiting an old material for new modes of energy conversion and CO_2 mitigation. *Phil. Trans. R. Soc. A* **368**: 3269–3294

[7] Ackermann, S., Sauvin, K., Castiglioni, R., Rupp, J. L. M., Scheffe, J. R., Steinfeld, A, (2015) Kinetics of CO_2 Reduction over Nonstoichiometric Ceria. *J. Physic. Chem. C* **119**: 16452-16461

[8] Coker, E. N., Ambrosini, A., Rodriguez, M. A., Miller, J. E. (2011) Ferrite-YSZ composites for solar thermochemical production of synthetic fuels: *in operando* characterization of CO_2 reduction. *J. Mater. Chem.* **21:** 10767

[9] Babiniec, S. M., Coker, E. N., Miller, J. E., Ambrosini, A. (2015) Investigation of LaSrCoMO (M = Mn, Fe) perovskite materials as thermochemical energy storage media. *Solar Energy* **118** 451-459

[10] Pechini, M. P. U.S. Patent 3,330,697. Method of preparing Lead and Alkaline Earth Titanites and Niobates and Coating Method Using the Same to Form a Capacitor. Filed August 26, 1963

[11] Huang, Y., Pellegrinelli, C., Geller, A., Liou, S., Jarry, A., *et al.* (2017) Direct observation of enhanced water and carbon dioxide reactivity on multivalent metal oxides and their composites. *Energy Environ. Sci.* **10**: 919.

[12] Mogensen, M., Lindegaard, T., Hansen, U. R. (1994) Physical Properties of Mixed Conductor Solid Oxide Fuel Cell Anodes of Doped CeO_2. *J. Electrochem. Soc.* **141**: 2122

[13] Mizusaki, J., Tagawa, H., Naraya, K., Sasamoto, T. (1991) Nonstoichoiometry and thermochemical stability of the perovskite-type $La_{1-x}Sr_xMnO_{3-d}$. *Solid State Ionics* **49**: 111-118